Noname manuscript No.
(will be inserted by the editor)

Oscillations and waves in solar spicules

T.V. Zaqarashvili · R. Erdélyi

Received: date / Accepted: date

Abstract Since their discovery, spicules have attracted increased attention as energy/mass bridges between the dense and dynamic photosphere and the tenuous hot solar corona. Mechanical energy of photospheric random and coherent motions can be guided by magnetic field lines, spanning from the interior to the upper parts of the solar atmosphere, in the form of waves and oscillations. Since spicules are one of the most pronounced features of the chromosphere, the energy transport they participate in can be traced by the observations of their oscillatory motions. Oscillations in spicules have been observed for a long time. However the recent high-resolutions and high-cadence space and ground based facilities with superb spatial, temporal and spectral capacities brought new aspects in the research of spicule dynamics. Here we review the progress made in imaging and spectroscopic observations of waves and oscillations in spicules. The observations are accompanied by a discussion on theoretical modelling and interpretations of these oscillations. Finally, we embark on the recent developments made on the presence and role of Alfvén and kink waves in spicules. We also address the extensive debate made on the Alfvén versus kink waves in the context of the explanation of the observed transverse oscillations of spicule axes.

Keywords 96.60.-j · 96.60.Na · 96.60.Mz

T.V. Zaqarashvili
Abastumani Astrophysical Observatory at the Faculty of Physics and Mathematics, I. Chavchavadze State University, Chavchavadze Ave. 32, Tbilisi 0179, Georgia
Tel.: +995-32-294714
Fax: +995-32-220009
E-mail: temury.zaqarashvili@iliauni.edu.ge

R. Erdélyi
Solar Physics & Space Plasma Research Centre (SP^{2}RC)
Department of Applied Mathematics
University of Sheffield
Sheffield S3 7RH, UK
E-mail: robertus@sheffield.ac.uk

1 Introduction

The rapid rise of plasma temperature up to 1 MK from the solar photosphere towards the corona is still an unresolved problem in solar physics. It is clear that the mechanical energy of sub-photospheric motions is transported somehow into the corona, where it may be dissipated leading to the heating of the ambient plasma. A possible scenario of energy transport is that the convective motions and solar global oscillations may excite magnetohydrodynamic (MHD) waves in the photosphere, which may then propagate through the chromosphere carrying relevant energy into the corona. It is of great desire that the energy transport process(es) can be tracked by observational evidence of the oscillatory phenomena in the chromosphere. For a detailed discussion about MHD wave heating and heating diagnostics in the solar atmosphere see the recent work by Taroyan and Erdélyi (2009).

Most part of the chromospheric radiation comes from *spicules*, which are grass-like spiky features seen in chromospheric spectral lines at the solar limb (see Fig 1). These abundant and spiky features in the chromosphere were discovered by Secchi (1877) and were named "spicules" by Roberts (1945). Beckers (1968, 1972); Sterling (2000) dedicated excellent reviews to summarizing the observational and theoretical views about spicules at that time. Since these reviews, many observational reports of *oscillatory phenomena in spicules* appeared in the scientific literature. In particular, it is anticipated that signatures of the energy transport by MHD waves through the chromosphere may be detectable in the dynamics of spicules. A comprehensive review summarizing the current views about the observed waves and oscillations in spicules, to the best of our knowledge, is still lacking and such a summary has not been published yet in the literature.

The goal of this review is to collect the reported observations about oscillations and waves in spicules, so that an interested reader could have a general view of the current standing of this problem. Here, we concentrate only on observed oscillatory and wave phenomena of spicules and their interpretations. We are not concerned about the models of spicule generation mechanisms; the interested reader may find these latter topics in the recent review by Sterling (2000) or in De Pontieu and Erdélyi (2006).

Section 2 is a short summary about the general properties of spicules, Section 3 describes the oscillation events reported so far for solar limb spicules, Section 4 outlines the views and discussions about the interpretation of spicule oscillations and Section 5 summarizes the main results and suggests future directions of research.

2 General properties of spicules

Spicules are grass-like structures in the solar lower atmosphere mostly detected in chromospheric Hα, D_3 and Ca II H lines. These spiky dynamic jets are propelled upwards (at speeds of about 20 km s^{-1}) from the solar surface (photosphere) into the magnetized low atmosphere of the Sun. According to early, but still valid estimates by Withbroe (1983) spicules carry a mass flux of about two orders of magnitude that of the solar wind into the low solar corona. With diameters close to observational limits (<500 km), spicules have been largely unexplained. The suggestion by De Pontieu et al. (2004) and De Pontieu and Erdélyi (2006) of channeling photospheric motion, i.e. the superposition of solar global oscillations *and* convective turbulence, has opened new avenues in the interpretation of spicule dynamics. The real strength of the observations

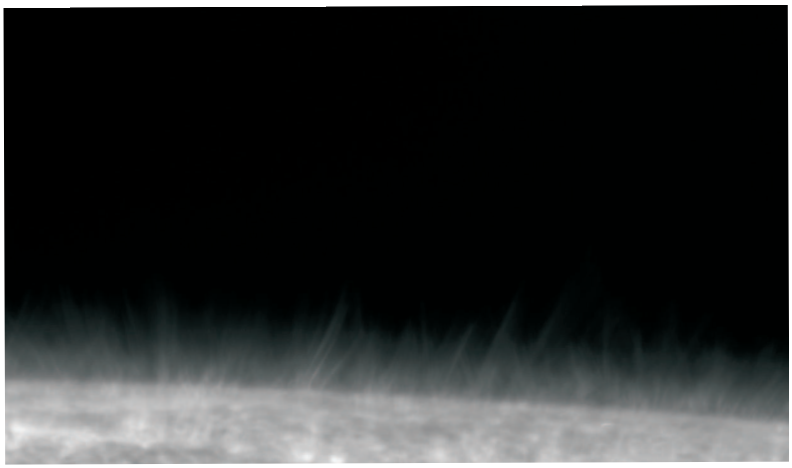

Fig. 1 High resolution image of spicules at the solar limb in Ca II H line taken by Solar Optical Telescope (SOT) on board of Hinode spacecraft (November 11, 2006).

and the forward modelling by De Pontieu and Erdélyi is that, none of the earlier existing models could account simultaneously for spicule ubiquity, evolution, energetics and the recently discovered periodicity (De Pontieu et al. (2003a,b)) of spicules.

Excellent summaries about the general properties of spicule have been presented almost forty years ago by Beckers (1968, 1972) and we broadly recall these findings here.

2.1 Diameter

Measured range of spicule diameter from ground based observations was $\sim$ 700-2500 km (Beckers (1968)). The general view was that the diameter varies from spicule to spicule having the values from 400 km to 1500 km. The spicules seemed to be wider in Ca II H line than in Hα (Beckers (1972)). However, the unprecedentedly high spatial resolution of Solar Optical Telescope on board of Hinode spacecraft (0.05 arc sec for Ca II H and 0.08 arc sec for Hα) revealed fine structure of spicules. Fig 1. shows this fine structure of spicules in Ca II H line at the solar limb taken by Hinode/SOT on November 11, 2006. The high resolution images revealed that the diameter of spicules is $\sim$ 150-400 km in Ca II H line and $\sim$ 350-400 km in Hα line (see also the high resolution image in Fig. 2 taken by Swedish Solar Telescope, courtesy De Pontieu et al. (2004)).

2.2 Length

The upper part of spicules continuously fade away with height, therefore the length is difficult to determine with precision. Generally, the top of a spicule is defined as the height where the spicule becomes invisible. The mean length of spicules varies from 5000 to 9000 km in Hα (Beckers (1972)). Recent Hinode/SOT observations (De Pontieu et al. (2007b)), however, revealed another type of spicules labelled as type II spicules. The length of these type II spicules is shorter, the values laying between 1000

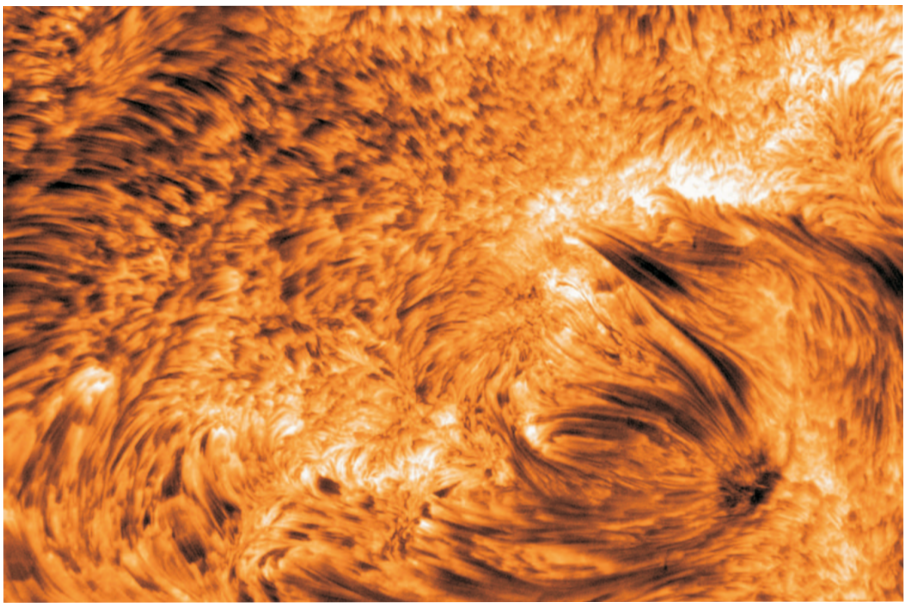

Fig. 2 High resolution image of spicules on solar disc taken by Swedish Solar Telescope (SST) in La Palma, adopted from De Pontieu et al. (2004).

and 7000 km. Additionally, very long spicules, called as *macrospicules* by Bochlin et al. (1975) with typical length of up to 40 Mm are frequently observed mostly near the polar regions as reported by e.g. Pike and Harrison (1997); Pike and Mason (1998); Banerjee et al. (2000); Parenti et al. (2002); Yamauchi et al. (2005); Doyle et al. (2005); Madjarska et al. (2006); O'Shea et al. (2005); Scullion et al. (2009); Nishizuka et al. (2009).

2.3 Temperature and Densities

Spicules have the temperatures and densities typical to the values of the chromospheric plasmas. Table 1 summarizes the typical electron temperatures (T_e) and number densities (n_e) of spicule values at different heights above the limb (Beckers (1968)). Caution has to be exercised as values at 2000 and 10000 km heights are unreliable because of insufficient data.

Table 1 Electron temperatures and densities inferred from spicule emission, after Beckers (1968)

h(km)	$T_e(K)$	n_e (cm^{-3})
2 000	17 000	22×10^{10}
4 000	17 000	20×10^{10}
6 000	14 000	11.5×10^{10}
8 000	15 000	6.5×10^{10}
10 000	15 000	3.5×10^{10}

2.4 Life time and motions

The change of spicule length has been studied by many authors (see Beckers (1972) and references therein). The general opinion is that spicules rise upwards with an average speed of 20-25 km/s, reach the height 9000-10000 km, and then either fade or descend back to the photosphere with the same speed. The typical life time of spicules is 5-15 mins, but some spicules may live longer or shorter. On the other hand, the type II spicules from Hinode/SOT have much shorter life time, about 10-150 s (De Pontieu et al. (2007b)). Measurements of Doppler shifts in spicule spectra revealed the velocity of 25 km/s, similar to the apparent speed, therefore it was suggested that the apparent motion is real. However, it is also possible that observed Doppler shifts partly correspond to the transverse motions of the spicule axis and not to the actual movement along the axis. Such transversal motions can be caused due to the propagation of e.g. waves in spicules. These periodic perturbations are the subject of our discussion in the remaining part of the paper.

3 Oscillations in solar limb spicules

Oscillations in solar limb spicules can be detected either by imaging or spectroscopic observations. Imaging observations may reveal the oscillations in spicule intensity and the visual periodic displacement of their axes. Imaging observations became especially important after the recently lunched Hinode spacecraft. SOT (Solar Optical Telescope) on board of Hinode gives unprecedented high spatial resolution images of chromosphere (see Fig. 1). On the other hand, the spectroscopic observations may give valuable information about spicules through the variation of line profile. Variations in Doppler shift of spectral lines can provide information about the line-of-sight velocity. Through spectral line broadening it is possible to estimate the non-thermal rotational velocities leading to the indirect observations of torsional Alfvén waves as suggested by Erdélyi and Fedun (2007), and reported recently by Jess et al. (2009) in the context of a flux tube connecting the photosphere and the chromosphere. Jess et al. used the technique of analysing Doppler-shift variations of spectral lines and detected oscillatory phenomena associated with a large bright point group, located near solar disk centre. Wavelet analysis reveals full-width half-maximum oscillations with periodicities ranging from 126 to 700 s originating above the bright point, with significance levels exceeding 99%. These oscillations, 2.7 km s^{-1} in amplitude, are coupled with chromospheric line-of-sight Doppler velocities with an average blue-shift of 23 km s^{-1}. The lack of co-spatial intensity oscillations and transversal displacements rule out the presence of magneto-acoustic wave modes. The oscillations are interpreted as a clear signature of torsional Alfvén waves, produced by a torsional twist of ± 25 degrees. A phase shift of 180 degrees across the diameter of the bright point suggests these Alfvén oscillations are induced globally throughout the entire brightening. The estimated energy flux associated with this wave mode seems to be sufficient for the heating of the solar corona, once dissipated.

Let us return to the possibility of intensity variations of spicules. Variation of line intensity indicates the propagation of compressible waves. And finally, the visible displacement of spicule axis may reveal the transverse waves and oscillations in spicules. Note that ground based coronagraphs can play an especially important role in spectroscopic observations.

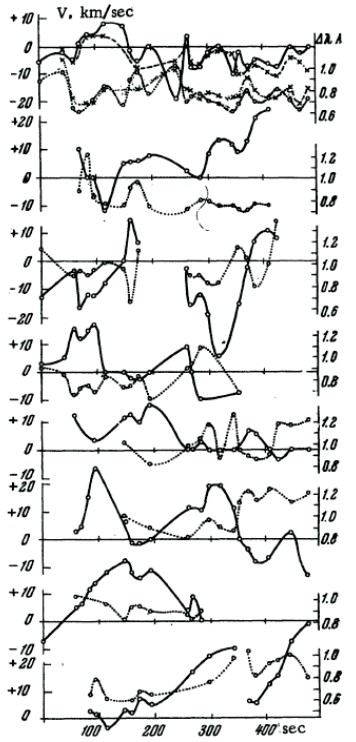

Fig. 3 Temporal variations in radial velocities (solid curves) and half widths (dotted curves) of 10 individual Hα spicules, adapted from Nikolsky and Sazanov (1967).

In this section we briefly outline almost all oscillation events in solar limb spicules reported so far in literature. Each observation is described in a separate subsection. At the end of the section, we summarize the information gathered about the typical observed periods in limb spicules.

3.1 Nikolsky and Sazanov (1967)

A very early, to the best of our knowledge the first, modern account of Doppler shift temporal variation in spicules was reported by Nikolsky and Sazanov (1967). A set of spectrograms of chromospheric spicules in Hα line were obtained with the coronagraph of the Institute of Terrestrial Magnetism (Russia) on 1 August 1964. The Hα profiles and radial velocities of 11 different spicules were successfully derived from successive Hα line spectra formed at a height of $\sim$6000 km above the solar limb. The time duration of observations was 8 mins with the intervals between exposures 10-40 s. Fig. 3 displays the time evolution of radial velocity and half width of Hα line for 10 different spicules. Quasi-periodic oscillations are clearly seen. The authors concluded that the radial velocities vary randomly with time with a mean period of $\sim$ 1 min. The amplitude of the oscillations are within 10-15 km/s. The half width of Hα line profile also tends to oscillate with a period similar to the mean period of $\sim$ 1 min.

3.2 Pasachoff et al. (1968)

Pasachoff et al. (1968) analyzed the high-dispersion spectra of the solar chromosphere obtained at the Sacramento Peak Observatory in several spectral regions separately during the summer of 1965. The observations were carried out simultaneously at two heights in the solar chromosphere separated by several thousands of kilometers.

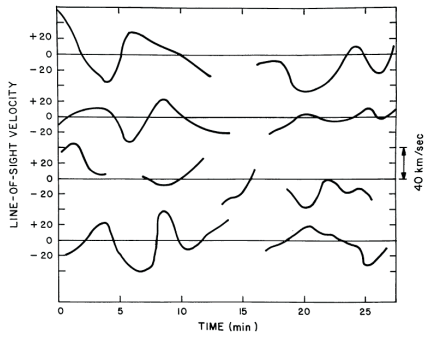

Fig. 4 Temporal variation of Doppler velocities in H-line of Ca II from Pasachoff et al. (1968).

The time series of Doppler velocities in H-line of ionized Calcium, Ca II, for 10 different spicules are shown in Fig. 4. The exposure time for H-line was 13 s, therefore the temporal resolution was sufficiently high. Also, a good spatial resolution with less than 2 arc sec was achieved. Pasachoff et al. (1968) were searching for the sign reversal of Doppler velocities in order to determine the rising/falling stages of spicule evolution. Indeed, some features show the sign reversal, but the common property is the clear quasi-periodic temporal variation of Doppler velocities with periods of 3-7 min. The amplitudes of oscillations are rather high, though still being within the range of 10-20 km/s. Pasachoff et al. (1968) interpreted the detected temporal variation as motion along the spicule axis, but transverse oscillations also cannot be ruled out.

3.3 Weart (1970)

Observations have been carried out with the Mount Wilson Solar Tower Telescope during the period of 10 September - 13 October, 1967. Time sequences of Hα spectra have been obtained corresponding to height 5000-6000 km height above the solar limb.

The author reported that, both Doppler velocity and horizontal motion of spicules as a whole have significant input into spicule dynamics. In at least two cases, the author found that the combined motion indicate movement of a gas in an arc of a horizontal circle, firstly towards the observer, followed by sideways, finally away. Weart concluded that only true transverse motion could explain the observed pattern of motion.

The power spectrum of temporal variations resembled the familiar 1/frequency curve, typical to many types of random motions. Substantial power was found to be concentrated at periods of 1, 2.5 and 10 minutes. However, no statistically significant peaks were observed. Therefore, it was concluded that spicules move horizontally at random.

3.4 Nikolsky and Platova (1971)

Detailed spectroscopic observations were carried out on 3 April 1969 with the 53 cm Lyot coronagraph mounted at the High Altitude Astronomical Station near Kislovodsk (Russia). 38 Hα spectrograms of the chromosphere were obtained during about a 21 minute observing campaign. The time interval between successive frames was 30 s on average, and the spatial resolution of observations was $\sim$ 1 arcsec. Two comparatively

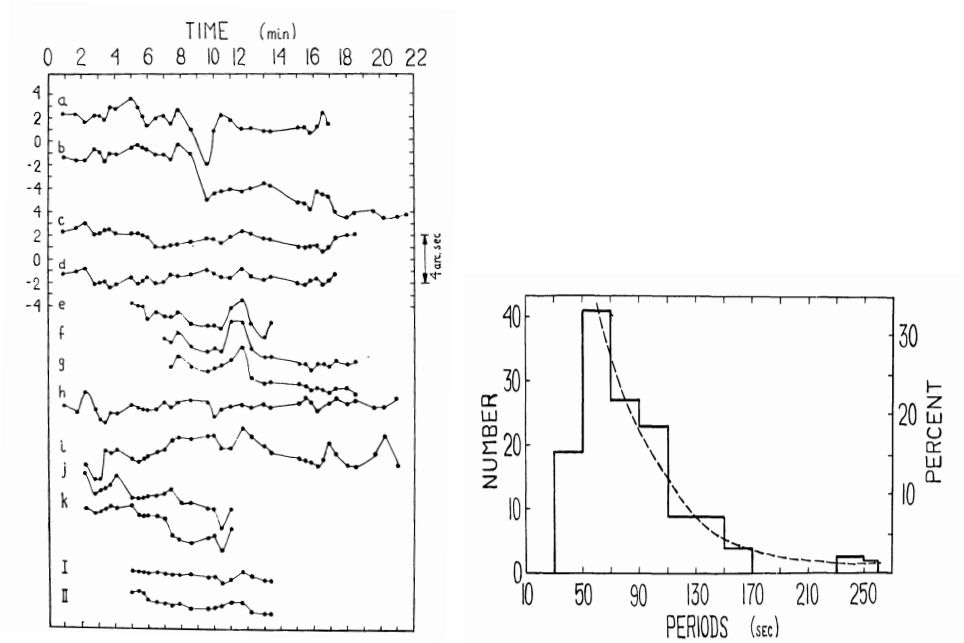

Fig. 5 Left: temporal variation of spicule positions along the solar limb, from Nikolsky and Platova (1971). Points denote the different positions of spicules during time series. I and II are the "bench-mark" spicules. Right: distribution of periods of spicule oscillations along the solar limb.

stable spicules, present in almost all frames, were chosen as reference ones. Then, the variation of other spicules along the limb with respect to these "bench-mark" spicules were determined. Fig. 5 (left panel) shows the position of several spicules vs time with respect to the "bench-mark" spicules. The oscillations of spicule position along the limb are clearly seen.

The distribution of periods of spicule oscillations along the limb is shown on the right panel of Fig. 5. The most probable period lies between 50-70 s and the authors concluded that spicules undergo transversal oscillations with a period of $\sim$ 1 min. The amplitude of oscillations was estimated to be about 10-15 km s^{-1}.

3.5 Kulidzanishvili and Nikolsky (1978)

The observational material described in the previous subsection was re-analyzed later by Kulidzanishvili and Nikolsky (1978) in order to search for a longer periodicity. The authors also searched for signatures of possible oscillations in Doppler velocity, line width and intensity, respectively. Fig. 6 shows the distribution of the spicule number

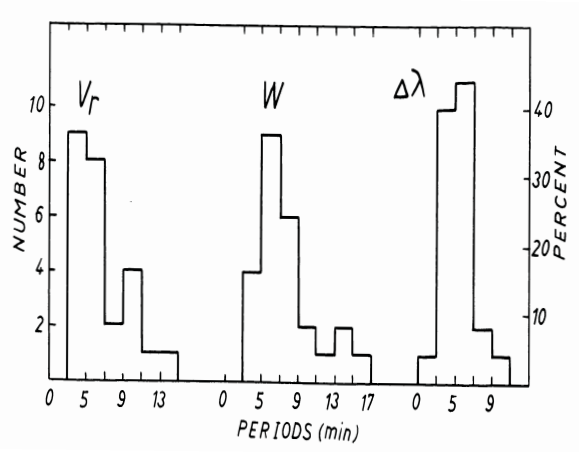

Fig. 6 Distribution of periods of Doppler velocity V_r, intensity W and full-width at half-maximum $\Delta\lambda$, adapted from Kulidzanishvili and Nikolsky (1978).

vs the observed periods of oscillation in line-of-sight velocity, line width and intensity. About 70% of the observed periods of Doppler shift oscillations are within 3-7 min. The same per cent of observed periods lies within 4-9 min in the spicule intensity and 80% of observed periods of line width oscillations are within 3-7 min.

3.6 Gadzhiev and Nikolsky (1982)

Observations were also carried out with the 53 cm Lyot coronagraph at Shemakha Astrophysical Observatory resulting in Hα time series corresponding to a height of 4 Mm above the solar limb. A total number of 15 spicules were investigated in details. Gadzhiev and Nikolsky analysed variations in Doppler velocity as well as in the tangential velocity, i.e. reflecting the visible displacement of spicule axes along the solar limb.

The authors found that the spicules oscillate with typical periods of 3-6 mins, both in line-of-sight and tangential directions. Fig. 7 shows the time variation of line-of-sight and tangential velocities in one of the spicules. The periodicity in both velocity components is clearly visible. Gadzhiev and Nikolsky also constructed the trajectories of spicule motion by putting together both velocity components. They concluded that spicules undergo a cyclic motion as a whole on an ellipse with an average period of 4 mins. The average amplitude of this cyclic motion was 11 km s^{-1}.

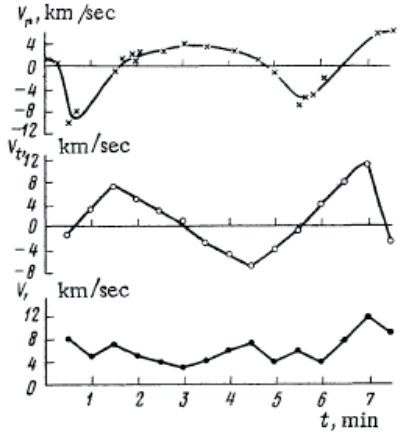

Fig. 7 Time variation of the radial and tangential velocities V_r, V_t and the modulus V of the velocity vector for a spicule, adapted from Gadzhiev and Nikolsky (1982).

3.7 Kulidzanishvili and Zhugzhda (1983)

Another spectroscopic observations were carried out with the 53 cm Lyot coronagraph mounted at the Abastumani Astrophysical Observatory (Georgia). A 22 minutes long time sequence, taken in the Hα line, was analyzed for a total number of 25 spicules. The statistically significant period of oscillations in intensity, line width and line-of-sight velocity was found to be $\sim$ 5 min.

3.8 Hasan and Keil (1984)

Observations were also carried out with the Vacuum Tower Telescope of the National Solar Observatory (USA) in the autumn of 1982. A set of Hα spectra corresponding to five slit positions above the solar limb were recorded every 8 s in order to investigate the temporal variations of spicules. The spatial resolution of these observations was better than 2 arcsec.

Hasan and Keil detected the temporal variations of the line-of-sight velocity at two different heights for two spicules. The fine time resolution allowed them to discern small amplitude fluctuations with periods of about 2-3 mins.

3.9 Papushev and Salakhutdinov (1994)

Observations were carried out with the 53 Lyot coronagraph of Sayan Observatory located near Irkutsk (Russia). The spectroscopic time series in different spectral lines varied from several minutes to hours with an excellent temporal resolution of 10-20 s. The spatial resolution of observations was better than 1 arcsec. The spectra were simultaneously registered at three different heights above the limb with a three-level image slicer.

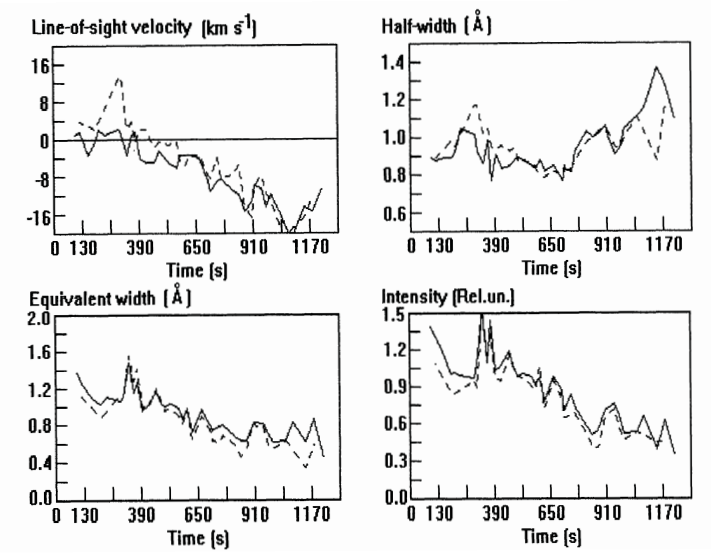

Fig. 8 Temporal variations of Hα line profile parameters and the line-of-sight velocity of spicules at different heights, adapted from Papushev and Salakhutdinov (1994). The solid line corresponds to the height of 5 Mm and the dashed line to 8 Mm above the solar limb, respectively.

Temporal variations of Hα line profile parameters and line-of-sight velocity for one of spicules at two different heights are shown on Fig.8. The quasi periodic fluctuations are clearly seen. Papushev and Salakhutdinov found that the oscillation periods lay between 80-120 sec.

3.10 Xia et al. (2005)

Xia et al. analyzed the time series of EUV spicules in two polar coronal holes obtained by the SUMER (Solar Ultraviolet Measurements of Emitted Radiation) camera on-board the SOHO (SOlar and Heliospheric Observatory) spacecraft. The spatial resolution of the observations was 1 arcsec and the exposure time for different data sets varied as 15, 30 and 60 s. Fig. 9 shows Dopplergrams and radiance map for the C III 977 Å line (left panel). The right panel shows the relative Doppler shifts at four different locations above the solar limb. The Doppler velocity and radiance indicate evidence of $\sim$5-min oscillations.

3.11 Kukhianidze et al. (2006)

Another, more recent observations were carried out on 26 September 1981 with the 53 cm Lyot coronagraph of the Abastumani Astrophysical Observatory (the instrumental spectral resolution and dispersion in Hα are 0.04 Å and 1 Å/mm correspondingly) at the solar limb. The scanning of height series began at the height of 3800 km measured from the photosphere, and continued upwards (Khutsishvili (1986)). The chromospheric Hα

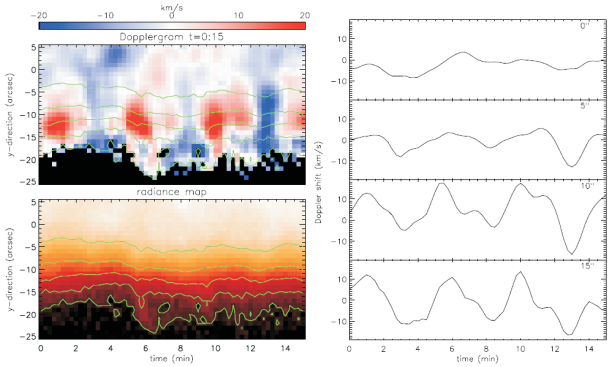

Fig. 9 Time series Dopplergram and radiance map for the C III 977 Å line showing levels of radiance in logarithmic scale (adapted from Xia et al. (2005)). The right panel shows the relative Doppler shift at four location above the limb.

line was used again to observe solar limb spicules at 8 different heights. The distance between neighbouring heights was $1''$ (which was the spatial resolution of observations), thus the distance of ∼3800-8700 km above the photosphere was covered. The exposure time was 0.4 s at four lower heights and 0.8 s at higher ones. The total time duration of each height series was 7 s. Consecutive height series began immediately, once a sequence was completed. Kukhianidze et al. (2006) analyzed the spatial distribution of Doppler

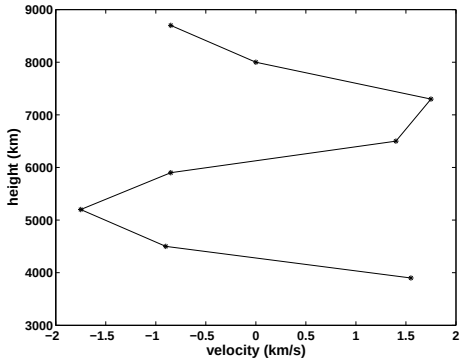

Fig. 10 The Doppler velocity spatial distributions for one of the height series from Kukhianidze et al. (2006). The marked dots indicate the observed heights.

velocities in selected Hα height series. Nearly 20% of the measured height series showed a periodic spatial distributions in the Doppler velocities. A typical Doppler velocity spatial distributions for one of the height series is shown in Fig. 10. A periodic spatial distribution is clearly seen. The authors suggested that the spatial distribution was caused by transverse kink waves. The wavelength was estimated to be ∼3.5 Mm. The period of waves were estimated to be in the range of 35-70 s.

3.12 Zaqarashvili et al. (2007)

Zaqarashvili et al. analysed the same observational data obtained by the 53 cm Lyot coronagraph of the Abastumani Astrophysical Observatory by Khutsishvili (1986). Using the height series, they constructed continuous time series of Hα spectra with an interval of ∼7-8 s between consecutive measurements at each height. The time series cover almost the entire lifespan (from 7 to 15 mins) of several spicules. Figure 11 shows

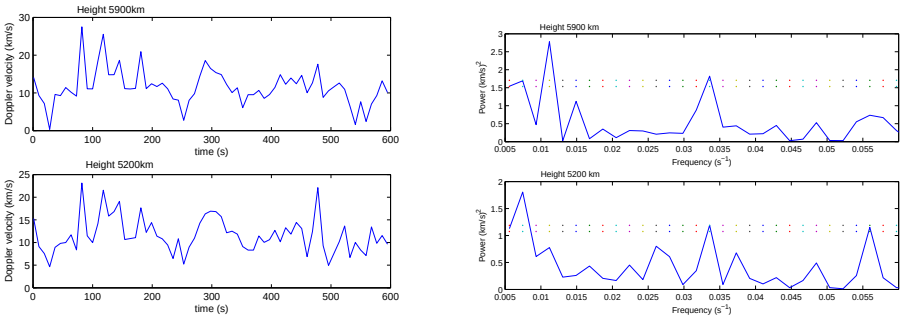

Fig. 11 Left: Doppler velocity time series at the heights of 5200 and 5900 km in one of the spicules, adapted from Zaqarashvili et al. (2007). The time interval between consecutive measurements is ∼8 s. Right: power spectra of Doppler velocity oscillations from the time series. The dotted lines in both plots show 95.5% and 98% confidence levels, respectively. There is the clear evidence of oscillations with periods of 180 and 30 s at both heights.

the Doppler velocity time series at two different heights above the solar limb in one of the spicules (left panel). The time series show the clear evidence of quasi-periodic oscillations in line-of-sight velocity. The power spectra resulted from Discrete Fourier Transform (DFT) analyses of the time series are presented in the right panel. The most pronounced periods at both heights are 180 and 30 s. The oscillation with the period of 90 s is also seen but preferably at higher heights (note the small peak at the lower height as well).

The power spectra of Doppler velocity oscillations in two other spicules at the heights of 5200 km (lower panels) and 5900 km (upper panels) are plotted on Figure 12.

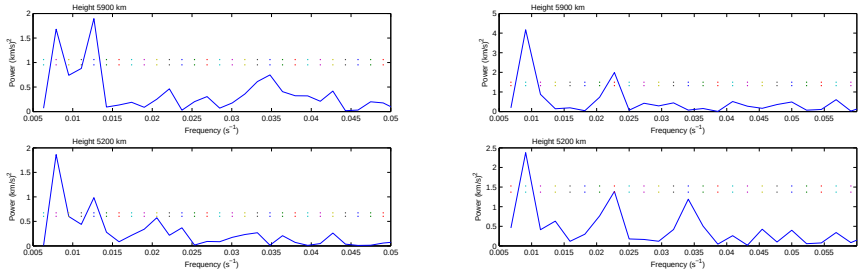

Fig. 12 Power spectra of Doppler velocity oscillations in another two spicules at the heights of 5200 and 5900 km (Zaqarashvili et al. (2007)). The dotted lines in both plots show 95.5% and 98% confidence levels.

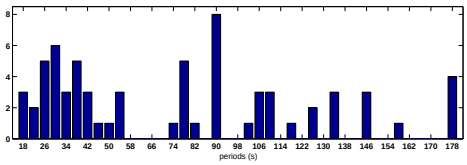

Fig. 13 Histogram of all oscillation periods that are above 95.5% confidence level, adapted from Zaqarashvili et al. (2007). The horizontal axis shows the oscillation periods in seconds, while the vertical axis shows the number of corresponding periods.

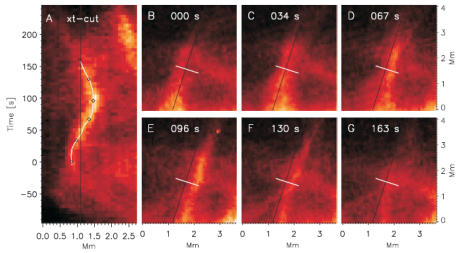

Fig. 14 An example of the transversal motion of a spicule obtained with Hinode/SOT by De Pontieu et al. (2007a). Panel A shows the intensity as a function of time along the spatial cut indicated by a white line on panels B-G. Panels B-G represent the time sequence of Ca II H images.

One of the spicules (left panels) shows the two clear oscillation periods of 120 and 80 s at both heights. Both periods are above the 98% confidence level. Another spicule undergoes oscillations with periods ∼110 and ∼40 s, respectively.

Zaqarashvili et al. also presented the results of DFT for 32 different time series as a histogram of all the oscillation periods above the 95.5% confidence level (see Figure 13). Almost half of the oscillatory periods are located in the period range of 18-55 s. Another interesting range of oscillatory periods is at 75-110 s, with a clear peak at the period of 90 s. Note that there is a further interesting period peak at 178 s as well, which is interpreted as a clear evidence of the well-known 3 min oscillations ubiquitous in the lower solar atmosphere.

3.13 De Pontieu et al. (2007a)

These authors analysed the time series of Ca II H-line images taken with SOT (Solar Optical Telescope) onboard the recently lunched Hinode satellite. SOT has high spatial (0.2 arcsec) and temporal (5 s) resolutions, and is capable of providing extremely useful information about the dynamics of the lower atmosphere.

De Pontieu et al. (2007a) found that many of the chromospheric spicules undergo substantial transverse displacements, with amplitudes of the order of 500 to 1000 km during their relatively short lifetime of 10 to 300 s. They also reported that some longer-lived spicules undergo periodic motions in a direction perpendicular to their axes. Fig. 14 shows an example of transverse displacement of a spicule with a period of ∼3 mins. In general, De Pontieu et al. (2007a) found it difficult to determine the periods of transverse motions due to the short life time of spicules. Fig. 15 shows the fine structure of spicules in Ca II H-line and the time-distance plot along the cut

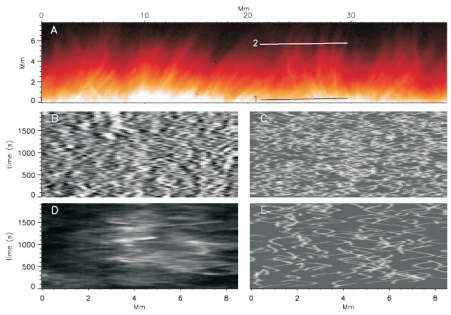

Fig. 15 Transverse motion of many spicules, from De Pontieu et al. (2007a). Panel A shows an image of the Hinode/SOT Ca II chromospheric line. Panels B and D are time-distance plots along the cuts labeled by 1 and 2 on panel A. Panels C and E are similar cuts but reproduced by Monte-Carlo numerical simulations of spicule motions.

parallel to the solar surface. The plots reveal the predominant linear motion of spicules rather than oscillatory ones. However, comparing these excellent quality observations to their Monte-Carlo simulations of numerically modelling swaying spicule motion, they suggested that the most expected periods of transverse oscillations should lay between 300 and 600 s, which they interpreted as signature of Alfvén waves.

3.14 Summary of observed oscillatory phenomena

All the observations allow us to make a short summary of oscillatory phenomena detected in limb spicules. The results are gathered in Table 2. Oscillations are more

Table 2 Summary of observed oscillatory periods in solar limb spicules

	Doppler velocity	visible displacement	intensity
Nikolsky and Sazanov (1967)	1 min	1 min	
Pasachoff et al. (1968)	3-7 min		
Weart (1970)	random	random	
Nikolsky and Platova (1971)		50-70 s	
Kulidzanishvili and Nikolsky (1978)	3-7 min		3-7 min
Gadzhiev and Nikolsky (1982)	3-6 min	3-6 min	
Kulidzanishvili and Zhugzhda (1983)	5-min		5-min
Hasan and Keil (1984)	2-3 min		
Papushev and Salakhutdinov (1994)	80-120 s	80-120	80-120
Xia et al. (2005)	5-min		5-min
Zaqarashvili et al. (2007)	30-110 s; 180 s		
De Pontieu et al. (2007a)		3 min; 300-600 s	

frequently observed in the Doppler velocity, which points towards transversal motions as the observations are performed at the solar limb. The longitudinal velocity component may also take a part in shaping the Doppler velocity oscillations as spicules are generally tilted away from the vertical. However, the transverse component seems to be the most important and determinant component in these oscillations as the visible displacement along the limb is also frequently reported. The observed periods can be

divided into two groups: those with shorter periods (<3-min) and those with longer periods $\geq$ 3-min. The most frequently observed oscillations are within the period ranges of $3 - 7$ min and $50 - 110$ s. The two, apparently separate groups of oscillations are probably caused by different physical mechanisms. Intensity oscillations are observed mostly with ∼5-min period, which may indicate their connection to the global photospheric 5-min oscillations (De Pontieu et al. (2003a,b, 2004); De Pontieu and Erdélyi (2006)). However, oscillations with other periods are probably connected with transverse displacement of spicule axes, which can be caused by kink or Alfvén waves. These possibilities are discussed later in details.

In order to infer more precise information about the oscillatory motions in the lower solar atmosphere, in particular in chromospheric spicules, it is of vital importance to determine whether the oscillations are caused by propagating or standing wave patterns. Unfortunately, this is a very challenging task from an observational perspective, and it is a difficult task from a theorist's point of view as well. To the best of our knowledge, very little is known about these mechanisms applicable to the highly stratified spicule geometry in the literature. Erdélyi et al. (2007) give an insight into the theoretical and numerical difficulties of studying waves and oscillations in the highly stratified lower solar atmosphere. In spite of these obstacles, some conclusions still can be drawn and we discuss them in the next section.

4 Propagation

The propagation of disturbances along spicules can be deduced when observations are performed at least at two different heights. Then the propagation speed can be estimated from the phase difference between oscillations at different heights.

Several authors reported the possible propagation speeds of disturbances in spicules. Pasachoff et al. (1968) found that velocity changes occur simultaneously, to within 20 s, at two distinct heights separated by 1800 km. They concluded that the propagation velocities should be more than 90 km s^{-1}. Hasan and Keil (1984) suggested the propagation of signals from lower to higher heights with an estimated velocity of more than 300 km s^{-1}. Papushev and Salakhutdinov (1994) studied the phase delays of fluctuations at different heights and also concluded that the propagation speeds should exceed 300 km s^{-1}. However, it must be noted that a standing oscillation pattern may also be responsible to explain these phenomena.

Detailed reports about wave propagation were presented by e.g. Kukhianidze et al. (2006) and Zaqarashvili et al. (2007) through analyzing the consecutive height series. Kukhianidze et al. (2006) presented three consecutive height series of Doppler velocities in a spicule, which show that the maximum of the Doppler velocity moves up in time (see Fig. 16). The authors suggested that this may indicate a wave phase propagation. The phase is displaced at ∼1500 km in about 18 s giving the phase speed of ∼80 km s^{-1}, very comparable to the expected kink or Alfvén speed at these heights.

Zaqarashvili et al. (2007) presented a Fourier power as a function of frequency and heights for two different spicules shown on Fig. 17 (left panel). There is clear evidence of persisting oscillations along the full length of both spicules. The plot of the first spicule shows the long white feature (feature A) located just above the frequency 0.01 s^{-1}. This is the oscillation with the period of ∼80 s and it persists along the spicule. The most pronounced feature (feature B) in the plot of the second spicule is colour-code indicated by a long brighter trend located just above the frequency of 0.02 s^{-1} and persisting

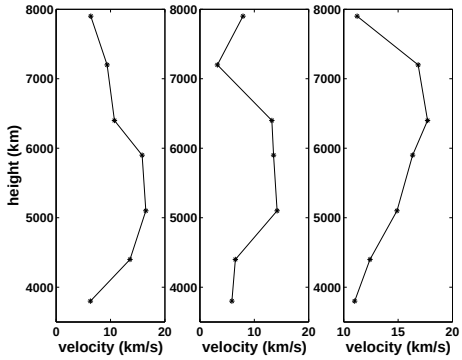

Fig. 16 Three consecutive height series of Doppler velocities in one of the spicules, adapted from Kukhianidze et al. (2006). The time difference between the consecutive plots is ∼8 s. The maximum of Doppler velocity moves up in consecutive height series, which most probably indicates wave propagation.

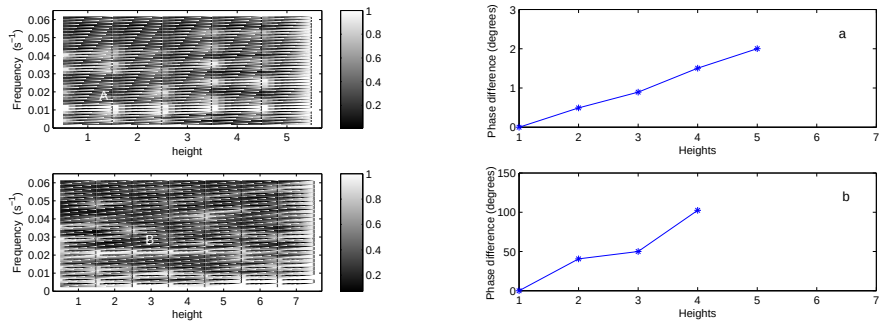

Fig. 17 Left: Fourier power expressed in confidence levels as function of frequency and heights for two different spicules, adapted from Zaqarashvili et al. (2007). Brighter points correspond to higher power, and darker points correspond to lower one. The label 1 on the power scale (right plots) corresponds to the level of 100% confidence. Right: Relative Fourier phase as a function of height for oscillations (a) with ∼80 s period in the first spicule (feature A) and (b) 44 s period in the second spicule (feature B). The distance between consecutive heights is ∼ 1 arc sec.

along almost the whole spicule. This is the oscillation with a period of 44 s. Then, Zaqarashvili et al. calculated the relative Fourier phase between heights for the most pronounced features (features A and B). Right panel of Figure 17 shows the relative Fourier phase as a function of heights for (a) feature A and (b) feature B. In spite of the apparent linear behaviour of the phase difference, there is practically almost no phase difference between oscillations at different heights for feature A, which probably indicates a standing-wave like pattern with period of ∼ 80-90 s. On the contrary, there is a significant linear phase shift in plot (b), which indicates a propagating pattern with an estimated period of ∼40-45 s. Therefore, the authors concluded that the first spicule shows the standing-wave like pattern (or a wave propagation almost along line of sight, which seems unlikely though cannot be ruled out) while the second spicule shows a propagating wave pattern. Zaqarashvili et al. estimated the propagation speed as ∼110 km s^{-1}.

Hence, based on these few observations we conclude that the propagation speed of disturbances in solar limb spicules is quiet high and may exceed 100 km s^{-1}. This indicates that the disturbances are of magnetic origin and they propagate with chromospheric Alfvén or kink speeds that exceeds the local sound speed at these heights.

5 Possible interpretation of observed oscillations

It is clear that the observed transverse oscillations of spicule axis can be explained and interpreted by the waves propagating along the spicule. The two type of waves responsible for periodic transverse displacement of spicule axis are: kink or Alfvén waves. If spicules are modelled as plasma jets being shoot along magnetic flux tube, then the transverse oscillations could be caused by MHD kink waves (Kukhianidze et al. (2006); Zaqarashvili et al. (2007); Erdélyi and Fedun (2007)). If a spicule is not stable wave guide for the tube waves, then the oscillations can be caused by Alfvén waves (De Pontieu et al. (2007a)). Before we embark on the interpretation of spicule oscillations, let us briefly summarise the possible MHD modes and their main properties in an inhomogeneous magnetised plasma under lower solar atmospheric conditions.

5.1 MHD waves in a uniform magnetic cylinder in the lower solar atmosphere

The magnetic building blocks in the solar atmosphere are the magnetic flux tubes. In a pioneering work by Edwin and Roberts (1983), using cylindrical coordinates, it was derived the dispersion relations of MHD waves propagating in cylindrical magnetic flux tubes. The main obstacle to be overcome when introducing the concept of flux tubes is the conversion from Cartesian to cylindrical coordinates. This change results involving Bessel functions in the dispersion relation which are not yet possible to be solved analytically without simplification, e.g. through incompressibility or long and short wavelength approximations. Let us summarise here the key steps of Edwin and Roberts (1983). Consider a uniform magnetic cylinder of magnetic field $B_0\hat{\mathbf{z}}$ confined to a region of radius a, surrounded by a uniform magnetic field $B_e\hat{\mathbf{z}}$ (see Figure 18a). To simplify the MHD equations we assume zero gravity, there are no dissipative effects and all the disturbances are linear and isentropic. Pressure (plasma and magnetic) balance at the boundary implies that

$$p_0 + \frac{B_0^2}{2\mu_0} = p_e + \frac{B_e^2}{2\mu_0}. \tag{1}$$

Linear perturbations about this equilibrium give the following pair of equations valid inside the tube,

$$\frac{\partial^2}{\partial t^2}\left(\frac{\partial^2}{\partial t^2} - (c_0^2 + v_A^2)\nabla^2\right)\Delta + c_0^2 v_A^2 \frac{\partial^2}{\partial z^2}\nabla^2\Delta = 0, \tag{2}$$

$$\left(\frac{\partial^2}{\partial t^2} - v_A^2\frac{\partial^2}{\partial z^2}\right)\Gamma = 0, \tag{3}$$

where ∇^2 is the Laplacian operator in cylindrical coordinates (r, ϕ, z) and

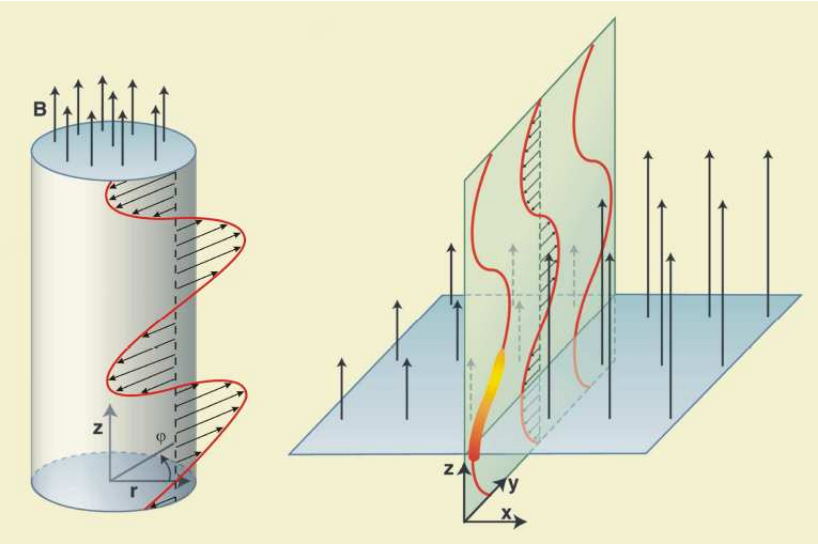

Fig. 18 *Left:* Magnetic flux tube showing a snapshot of Alfvén wave perturbation propagating in the longitudinal z-direction along field lines at the tube boundary. At a given height the Alfénic perturbations are torsional oscillations, i.e. oscillations are in the φ-direction, perpendicular to the background field. Note that on the other hand MHD kink waves would force the tube axis to oscillate. *Right:* Snapshot showing Alfvén waves propagating along a magnetic discontinuity. Again, the key feature to note is that Alfvénic perturbations are *within* the magnetic surface (yz-plane) at the discontinuity, perpendicular to the background field (y-direction), while the waves themselves propagate along the field lines (z-direction). The MHD kink waves oscillate in xz-plane in this geometry. Image adapted from Erdélyi and Fedun (2007).

$$\Delta \equiv \mathrm{div}\mathbf{v}, \quad \Gamma = \hat{\mathbf{z}} \cdot \mathrm{curl}\mathbf{v} \tag{4}$$

for velocity $\mathbf{v} = (v_r, v_\phi, v_z)$. A similar pair of equations to (2) and (3) are valid outside the tube. Fourier analysing we let

$$\Delta = R(r) exp[i(\omega t + n\phi + kz). \tag{5}$$

Then equations (2) and (3) give Bessel's equation satisfied by $R(r)$ as follows

$$\frac{\mathrm{d}^2 R}{\mathrm{d}r^2} + \frac{1}{r}\frac{\mathrm{d}R}{\mathrm{d}r} - \left(m_0^2 + \frac{n^2}{r^2}\right) R = 0, \tag{6}$$

where

$$m_0^2 = \frac{(k^2 c_0^2 - \omega^2)(k^2 v_A^2 - \omega^2)}{(c_0^2 + v_A^2)(k^2 c_T^2 - \omega^2)}. \tag{7}$$

We have used the notation v_A for the Alfvén speed and c_T for the characteristic tube speed (sub-Alfvénic), where $c_T = c_0 v_A/(c_0^2 + v_A^2)^{-1/2}$. To obtain a solution to (6) bounded at the axis ($r = 0$) we must take

$$R(r) = A_0 \left\{ \begin{array}{l} I_n(m_0 r),\ m_0^2 > 0 \\ J_n(n_0 r),\ n_0^2 = -m_0^2 > 0 \end{array} \right\} (r < a), \tag{8}$$

where A_0 is an arbitrary constant and I_n, J_n are Bessel functions, see e.g. Abramowitz and Stegun (1967), of order n. For a mode locked to the waveguide it is required that no energy propagates to or from the cylinder in the external region, i.e. the waves are evanescent outside the flux tube. Therefore we take

$$R(r) = A_1 K_n(m_e r), \quad r > a, \tag{9}$$

where A_1 is a constant and

$$m_e^2 = \frac{(k^2 c_e^2 - \omega^2)(k^2 v_{Ae}^2 - \omega^2)}{(c_e^2 + v_{Ae}^2)(k^2 c_{Te}^2 - \omega^2)}, \tag{10}$$

which is taken to be positive (no leaky waves). Since we must have continuity of velocity component v_r and total pressure at the cylinder boundary $r = a$, this yields the dispersion relations

$$\rho_0 (k^2 v_A^2 - \omega^2) m_e \frac{K_n'(m_e a)}{K_n(m_e a)} = \rho_e (k^2 v_{Ae}^2 - \omega^2) m_0 \frac{I_n'(m_0 a)}{I_n(m_0 a)}, \tag{11}$$

for surface waves ($m_0^2 > 0$) and

$$\rho_0 (k^2 v_A^2 - \omega^2) m_e \frac{K_n'(m_e a)}{K_n(m_e a)} = \rho_e (k^2 v_{Ae}^2 - \omega^2) n_0 \frac{J_n'(n_0 a)}{J_n(n_0 a)}, \tag{12}$$

for body waves ($m_0^2 = -n_0^2 < 0$). The axisymmetric sausage mode is given by $n = 0$, while the well-observed kink mode (non-axisymmetric) is given by $n = 1$. Modes with $n > 1$ are called flute modes. Although the dispersion relations (11) and (12) are complicated, finding the phase speed for e.g. kink waves with photospheric parameters simplifies matters considerably.

Under lower solar atmospheric conditions, characterised by $c_e > v_A > c_0$, possibly representative for spicules, sunspots or pores both the slow and fast bands have surface and body modes, respectively. The slow MHD waves are in a narrow band since $c_0 \approx c_T$. The slow body waves are almost non-dispersive, whereas the almost identical slow surface sausage and kink modes are weakly dispersive (bottom zoomed out panel in Fig. 19). On the other hand, if the characteristic speeds of a lower solar atmospheric flux tube render as $v_A > c_e > c_0$, the fast body modes do not exist since they would become leaky mode solutions of the dispersion relations (11)-(12). The MHD modes propagating along the flux tube in this case are shown in Fig. 20. Note, there is little evidence, whether flux tubes modelling spicules, are characterised by $c_e > v_A > c_0$ or $v_A > c_e > c_0$. In fact, it could be that closer to the solar photosphere the earlier characteristic speed rendering is valid, while higher up in the chromosphere the latter one is a better model determining wave modes and their propagation. In the incompressible limit, suitable for the description of kink waves and oscillations in their linear limit, $(c_0^2 \to \infty, c_e^2 \to \infty), m_0$ and m_e become $|k|$. The kink and sausage modes are then given explicitly after some algebra. It is noted that the phase speed for the kink mode is not monotonic as a function of k but has a maximum/minimum and the sausage mode is monotonically increasing/decreasing. This max/min feature of the kink mode is absent in the slab case, so it can be deduced to be a reflection of the geometry of the

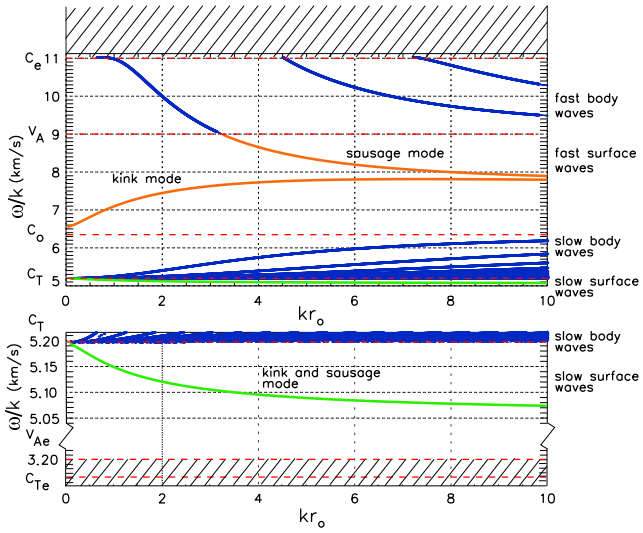

Fig. 19 The solution of the dispersion relations (11)-(12) in terms of phase speed (ω/k) of modes under photospheric conditions $c_e > v_A > c_0$ (all speeds are in km/s). The slow band is zoomed (lower panel). Image adapted from Erdélyi (2008).

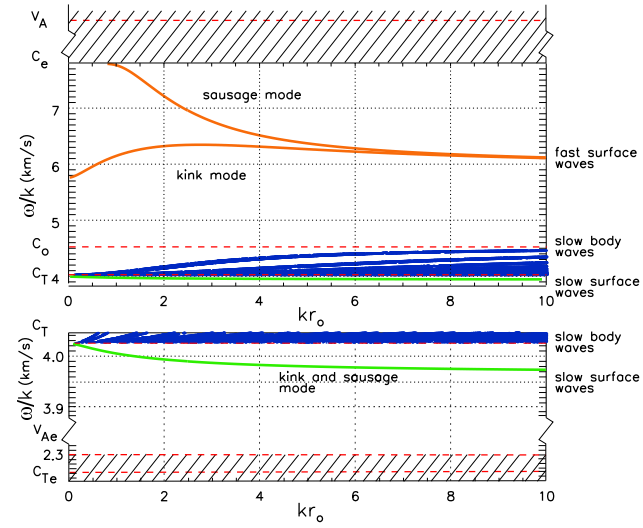

Fig. 20 Similar to Fig. 19 but for $v_A > c_e > c_0$. Image adapted from Erdélyi (2008).

magnetic field. On the other hand, the incompressible Alfvén waves in magnetic tubes are polarized in the ϕ direction and do not lead to the displacement of the tube axes (see Figure 18a).

Last but not least, for completeness and for the benefit of interested readers, we note

that kink MHD wave propagation under solar coronal conditions is discussed in details by Ruderman and Erdélyi (2009) in this Volume.

5.2 MHD kink waves

Equipped with a clear understanding of the differences between kink and Alfvénic perturbations, as described above, let us now return to plausible interpretations of periodic spicular motions. If spicules are formed in thin magnetic flux tubes and the MHD wave theory applies in *some* format as outlined in the Sec. 5.1, then the observed periodic transverse displacement of the axis probably is due to the propagation of kink waves (see Figs. 18 and 21). Transverse kink waves can be generated in photospheric magnetic tubes by buffeting of granular motions (Roberts (1979); Spruit (1981); Osin et al. (1999)). The waves may then propagate through the stratified chromosphere (see, e.g. Hargreaves (2008); Hargreaves and Erdélyi (2009)) and lead to the observed oscillations (Kukhianidze et al. (2006); Zaqarashvili et al. (2007)). If the velocity of the kink wave is polarized in the plane of observation, then it results in the Doppler shift of the observed spectral line (Nikolsky and Sazanov (1967); Pasachoff et al. (1968); Kulidzanishvili and Nikolsky (1978); Gadzhiev and Nikolsky (1982); Kulidzanishvili and Zhugzhda (1983); Hasan and Keil (1984); Papushev and Salakhutdinov (1994); Xia et al. (2005); Kukhianidze et al. (2006); Zaqarashvili et al. (2007)). However, if the velocity is polarized in the perpendicular plane then it results the visible displacement of spicule axis along the limb (Nikolsky and Sazanov (1967); Nikolsky and Platova (1971); Gadzhiev and Nikolsky (1982); Papushev and Salakhutdinov (1994)). Kink wave

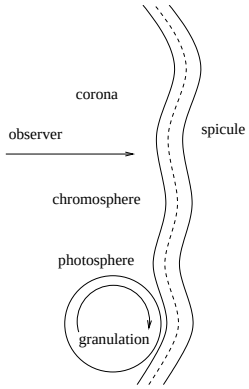

Fig. 21 Schematic picture of propagating kink waves in spicules, adapted from Kukhianidze et al. (2006).

propagation along a vertical thin magnetic flux tube embedded in the *stratified* field-free atmosphere is governed by the Klein-Gordon equation (Rae and Roberts (1982); Spruit and Roberts (1983); Hasan and Kalkofen (1999); Zaqarashvili and Skhirtladze (2008); Hargreaves (2008); Hargreaves and Erdélyi (2009); the latter authors have even considered a dissipative medium resulting in a governing equation of the type of Klein-

Gordon-Burgers equation)

$$\frac{\partial^2 Q}{\partial z^2} - \frac{1}{c_k^2}\frac{\partial^2 Q}{\partial t^2} - \frac{\Omega_k^2}{c_k^2} Q = 0, \tag{13}$$

where $Q = \xi(z,t)\exp(-z/4\Lambda)$, $c_k = B_0/\sqrt{4\pi(\rho_0+\rho_e)}$ is the kink speed, Λ is the density scale height and $\Omega_k = c_k/4\Lambda$ is the gravitational cut-off frequency for isothermal atmosphere (temperature inside and outside the tube is assumed to be the same and homogeneous). Here $\xi(z,t)$ is the transversal displacement of the tube, $B_0(z)$ is the tube magnetic field, $\rho_0(z)$ and $\rho_e(z)$ are the plasma densities inside and outside the tube respectively (the magnetic field and densities are functions of z, while the kink speed c_k is constant in the isothermal atmosphere).

Eq. (13) yields simple harmonic solutions $\exp[i(\omega t \pm k_z z)]$ with the dispersion relation

$$\omega^2 - \Omega_k^2 = c_k^2 k_z^2, \tag{14}$$

where ω is the wave frequency and k_z is the wave number. The dispersion relation shows that waves with higher frequency than Ω_k may propagate in the tube, while the lower frequency waves are evanescent.

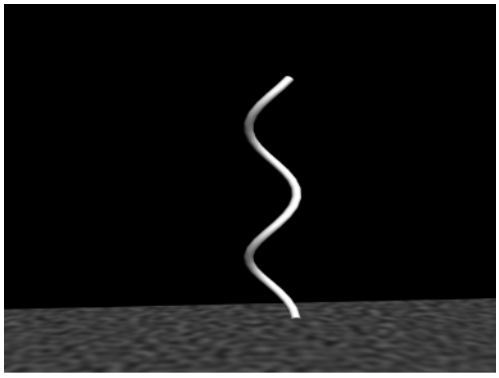

Fig. 22 Helical kink wave in a thin magnetic flux tube, adapted from Zaqarashvili and Skhirtladze (2008).

Kink waves cause the transverse displacement of the entire tube. The displacement of tube in a simple harmonic kink wave is polarized arbitrarily and the polarization plane depends on the excitation source. The superposition of two or more kink waves polarized in different planes may give rise to the complex motion of the tube. The process is similar to the superposition of two plane electromagnetic waves, where the waves with the same amplitudes lead to the circular polarization, while the waves with different amplitudes lead to the elliptical polarization. Consider, for example, two harmonic kink waves with the same frequency but polarized in the xz and yz planes: $A_x = A_{x0}\cos(\omega t + k_z z)$ and $A_y = A_{y0}\sin(\omega t + k_z z)$. The superposition of these waves sets up *helical waves* with a circular polarization if $A_{x0} = A_{y0}$ (Zaqarashvili and Skhirtladze (2008)). As a result, the tube axis rotates around the vertical, while the displacement remains constant (Fig. 22). If $A_{x0} \neq A_{y0}$ then the resulting wave

is elliptically polarized. The superposition of few harmonics with different frequencies and polarizations may lead to an even more complex motion of the tube axis.

5.3 Alfvén waves

De Pontieu et al. (2007a) suggested that the transverse displacement of spicule axis can be explained by the propagation of Alfvén waves excited in the photosphere by granular motions or global oscillation patterns. They performed self-consistent 3D radiative MHD simulations ranging in the vertical direction from the convection zone up to the corona. A snapshot from the simulations is presented on the Fig. 23 (panel A). Their analysis shows that the field lines (red lines) in the corona, transition region, and chromosphere are continuously shaken and carry Alfvén waves. Panels B and C are time-distance plots from the simulations and observations, respectively. From the comparison between simulations and observations the authors concluded that the period of Alfvén waves should lay between 100 and 500 s. However, they suggested that very long-lived macro spicules show some evidence of Alfvén waves with longer periods between 300 and 600 s. De Pontieu et al. (2007a) also claim that their simulations do not show the spicules as stable wave guide for kink waves. Therefore they argue that volume-filling Alfvén waves cause the swaying of magnetic field lines back and forth leading to the visible displacement of spicule axis. These claims are debated by Erdélyi and Fedun (2007): "However, these observations also raise concerns about the applicability of the classical concept of a magnetic flux tube in the apparently very dynamic solar atmosphere, where these sliding jets were captured. In a classical magnetic flux tube, propagating Alfvén waves along the tube would cause torsional oscillations (see Fig. 18a in this paper earlier). In this scenario, the only observational signature of Alfvén waves would be spectral line broadening. Hinode/SOT does not have the appropriate instrumentation to carry out line width measurements. On the other hand, if these classical flux tubes did indeed exist, then the observations of De Pontieu et al. (2007a) would be interpreted as kink waves (i.e., waves that displace the axis of symmetry of the flux tube like an S-shape). More detailed observations are needed, perhaps jointly with STEREO, so that a full three-dimensional picture of wave propagation would emerge."

5.4 Kink vs Alfvén waves

It is important to determine accurately which type of waves are responsible for the transverse displacement of the tube axis (Erdélyi and Fedun (2007); Jess et al. (2009)). The existence and main features of wave modes depend on the properties of the medium where the waves propagate in (see Sec. 5.1). If spicules represents a magnetic flux tube, then MHD wave theory may permit the propagation of kink and torsional Alfvén waves. The kink waves are global tube waves and cause the displacement of the tube as a whole. However, most importantly let us emphasise once more that torsional Alfvén waves do not lead to the displacement of tube axis (Erdélyi and Fedun (2007); Van Doorsselaere et al. (2008); Jess et al. (2009)). Therefore, torsional Alfvén waves are unlikely to be the reason for the observed oscillations. However, *global* Alfvén waves, which may indeed fill a significant volume in and around spicules, may cause the global transverse oscillations of magnetic field lines. In this latter scenario spicules may just

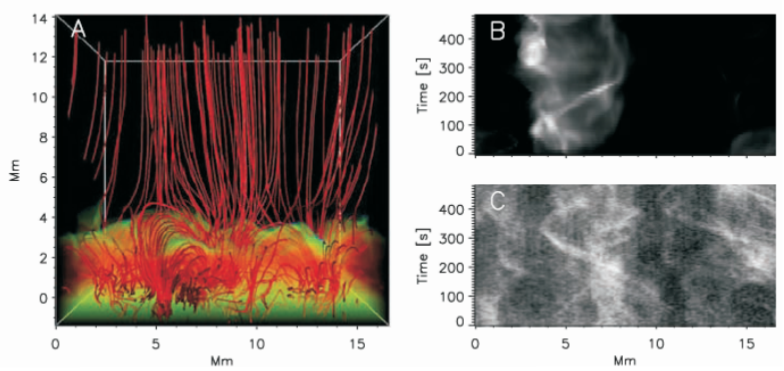

Fig. 23 Comparison between observations and simulations of Alfvén waves from De Pontieu et al. (2007a). A: a snapshot from 3D radiative MHD simulation. B: space-time plot from simulations. C: space-time cut from observations.

simply follow the oscillations of field lines and this is what De Pontieu et al. (2007a) may suggest.

However, there are two difficulties associated with the Alfvén wave scenario. Firstly, if the oscillations of spicules are due to global Alfvén perturbations, then the neighbouring spicules should show a coherent oscillation. However, Hinode movies indicate the opposite, i.e. spicule movements are random and there is no sign of coherent oscillations. Secondly, it is not yet clear how the volume-filling Alfvén waves would be generated in the photosphere, where the magnetic field is rooted and concentrated in flux tubes. In this regards, it seems to be more plausible that granular motions cause the transverse displacement of tube axis, that propagates then upwards in the form of kink waves. Such waves may lead to the observed oscillations of the spicule axis (see e.g. Zaqarashvili and Skhirtladze (2008)).

It must be noted as well that, the kink wave scenario also has its own difficulties as the photospheric flux tubes may be expanded in the chromosphere. This expansion may cause certain difficulties for the kink wave to propagate. For the recently developed theory of transversal waves and oscillations in gravitationally and magnetically stratified flux tubes see, e.g. Verth and Erdélyi (2008); Ruderman et al. (2008); Andries et al. (2009). Kink waves in expanding and stratified flux tubes may be transformed into Alfvén-like waves in the chromosphere, where the magnetic field rapidly expands, possibly leading to the diffusion of tubes. On the other hand, Hinode/SOT movies show tube-like behavior of spicules although De Pontieu et al. (2007a) could not found the spicules as stable wave guides of kink waves in their numerical simulations. In the contrary, Erdélyi and Fedun (2007), in the context of prominence oscillations, showed that kink waves can be easily guided. The problem whether the spicule displacements are Alfvénic or kink waves is currently under debate and more sophisticated observations complemented by numerical investigations are needed for a satisfactory solution (Erdélyi and Fedun (2007)).

5.5 Transverse pulse

It must be recognised that simple harmonic waves can hardly be excited in the dynamic solar photosphere. A more realistic process of wave excitation is the impulsive buffeting of granules on an anchored magnetic flux tube, which may easily generate transverse pulses. Such pulses may propagate upwards in the stratified atmosphere and leave the "wake" oscillating at cut -off frequency of kink waves (Zaqarashvili and Skhirtladze (2008)). The wake may be also responsible for the observed transverse oscillations of spicule axes.

For the sake of simplicity, let us consider the simplest impulsive forcing in both time and coordinate. Then Eq. (13) looks as (Zaqarashvili and Skhirtladze (2008))

$$\frac{\partial^2 Q}{\partial z^2} - \frac{1}{c_k^2}\frac{\partial^2 Q}{\partial t^2} - \frac{\Omega_k^2}{c_k^2} Q = -A_0 \delta(t)\delta(z), \tag{15}$$

where $z > -\infty$, $t > 0$, A_0 is a constant and the pulse is set off at $t = 0$, $z = 0$.

The solution of this equation can be written, after e.g. (Morse and Feshbach (1953)),

$$Q = A_0 c_k \delta\left(t - \frac{z}{c_k}\right) - \frac{c_k A_0}{2} J_0\left[\Omega_k \sqrt{t^2 - \frac{z^2}{c_k^2}}\right] H\left[\Omega_k\left(t - \frac{z}{c_k}\right)\right], \tag{16}$$

where J_0 and H are Bessel and Heaviside functions, respectively. Eq. (16) shows that the wave front propagates with the kink speed c_k (the first term), while the wake oscillating at the cut-off frequency Ω_k is formed behind the wave front (the second term) and it decays as time progresses (Rae and Roberts 1982; Spruit and Roberts 1983; Hasan and Kalkofen 1999; Hargreaves 2008; Hargreaves and Erdélyi 2009). Note, the actual mathematical form of the governing equation and its solution for kink and longitudinal oscillations in a gravitationally stratified and anchored magnetic flux tube is very similar, see e.g. Sutmann et al. (1998); Musielak and Ulmschneider (2001); Ballai et al. (2006) for more details.

Fig. 24 shows the plot of the transverse displacement $\xi(z,t) = Q(z,t)\exp(z/4\Lambda)$, where Q is expressed by the second term of Eq. (16). A rapid propagation of the pulse is found, which is followed by the oscillating wake (the time is normalized by the cut-off period $T_k = 2\pi/\Omega_k$). Just after the propagation of the pulse, the tube begins to oscillate with the cut-off period at each height. The amplitudes of pulse and wake increase upwards due to the density reduction, but the oscillations at each height decay in time. A very similar and resembling behaviour was found by Fleck and Deubner (1989); Fleck and Schmitz (1991); Schmitz and Fleck (1998); Erdélyi et al. (2007); Malins and Erdélyi (2007) for longitudinal oscillations.

Hence, the transverse and impulsive action on the magnetic tube at $t = 0$ near the base of the photosphere (as set at $z = 0$) excites the upward propagating kink pulse, while the tube in the photosphere oscillates at the photospheric kink cut-off frequency, Ω_k, which depends on the plasma-β parameter ($= 8\pi p_0/B_0^2$) inside the tube. In the case of a temperature balance inside and outside the tube, the kink speed can be expressed as $c_k = c_s[\gamma(1+2\beta)/2]^{-1/2}$, where c_s is the sound speed and γ is the ratio of specific heats ($\gamma = 5/3$ for adiabatic process). Then, the photospheric sound speed of 7.5 km s^{-1} and $\beta = 0.3$ gives 6.5 km s^{-1} for the kink speed. Consequently, we may estimate the kink cut-off period as $\sim$8 min, using the photospheric scale height of 125 km. Hence, the magnetic tube will oscillate with $\sim$8 min period in the photosphere.

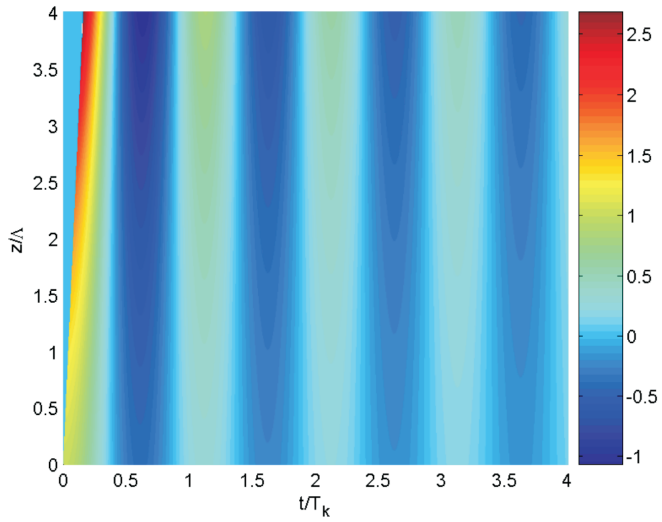

Fig. 24 Propagation of transverse kink pulse in stratified vertical magnetic flux tubes, adapted from Zaqarashvili and Skhirtladze (2008). A rapid propagation of the pulse is seen, which is followed by the oscillating wake. The pulse propagates with the kink speed and the wake oscillates with the cut-off period. The amplitude of the pulse (and wake) increases with height due to the decreasing density.

When the pulse penetrates into the higher chromosphere, where the cut-off period is changed, this will influence the propagation of the pulse. Spicules with higher density concentrations than the ambient plasma may guide kink waves with the phase speed of 25 km/s, which yields the cut-off period of about 500 s. Note, the Alfvén cut-off period can be as short as 250 s. Therefore, the transverse pulse may set up the oscillating wake in the chromosphere with the period of 250-500 s.

It is most likely, that the anchored magnetic flux tube undergoes granular buffeting from different sides. Therefore, the first pulse polarized, say, in yz can be rapidly followed by another pulse polarized in another plain. The second pulse rapidly propagates upwards and leaves another wake, which oscillates with the same cut-off frequency, but the oscillation is polarized in the xz plain. Hence, there are two transverse oscillations with the same frequency, but polarized in perpendicular planes. The superposition will set up a helical motion of the tube axis with the cut-off period (Zaqarashvili and Skhirtladze (2008)). The helical motion of spicule axis first has been observed by Gadzhiev and Nikolsky (1982) from simultaneous observation of Doppler velocity and visual displacements. The recent Hinode/SOT movies also show complex motions of spicule axis. Fig. 25 (upper panels) show the observed trajectories of spicule axis with respect to the photosphere, adopted from Gadzhiev and Nikolsky (1982). The lower panel shows the superposition of two wakes at the height of 250 km above the photosphere, numerically simulated by Zaqarashvili and Skhirtladze (2008), by solving the Klein-Gordon governing equation. The first wake corresponds to the pulse imposed along the x-direction and the second wake is the result of another pulse generated in the y-direction with a different amplitude. The observed period of helical motions is in the range of 3-6 mins, which may correspond well with the kink cut-off period in the chromosphere. A very

similar phenomenon was recently observed in fibril orientation by Koza et al. (2007). Therefore, the oscillation of wakes behind a transverse pulse may easily explain the

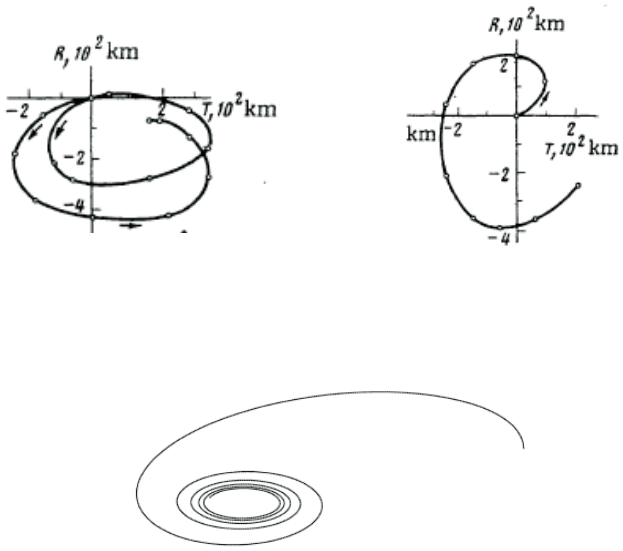

Fig. 25 Upper panels: Observed trajectories of the motion of two distinct spicules, adapted from Gadzhiev and Nikolsky (1982). Lower panel: Simulated helical motion of the tube axis at the height of 250 km measured from the solar surface, due to the propagation of two consecutive transverse pulses polarized in perpendicular planes, adapted from Zaqarashvili and Skhirtladze (2008).

visible transverse displacement of spicule axis observed by De Pontieu et al. (2007a) with Hinode/SOT. The cut-off period is similar or slightly shorter than the mean life time of spicules, therefore the oscillations are difficult to detect as it is noted by De Pontieu et al. (2007a).

6 Summary of main results and targets for future work

Spicules are one of the most plausible tracers and trackers of the energy coupling and energy transport from the lower solar photosphere towards the upper corona by means of MHD waves. These waves may induce the oscillatory phenomena in the chromosphere, which are frequently detected in limb spicules. Periodic perturbations, e.g. in forms of oscillations, are observed by both spectroscopic and imaging observations. Let us summarize the main observed oscillatory phenomena (see also Table 2):

- Oscillations in limb spicules are more frequently observed in Doppler shifts and in the visible displacement of spicule axis, which probably indicate the presence of transversal motions of spicules as a whole.
- The observed oscillation periods can be divided into two main groups: those with shorter (<3-min) and those with longer (≥3-min) periods.

- The most frequently observed oscillations are with period ranges of $50 - 110$ s and $3 - 7$ min.
- The propagation of the actual oscillations is rather difficult to detect. However, the relative Fourier phase between oscillations at different heights indicates the propagation speed of ~ 110 km s^{-1}. In some oscillations, perhaps caused by standing patterns, waves seem to be present with very high phase speeds (> 300 km s^{-1}).

The observed oscillations in spicules are most likely due to the propagation of transverse waves from the photosphere towards the corona. There are several possible interpretations of these oscillatory phenomena:

- Kink waves propagating along slender magnetic flux tubes, where spicules are formed on field lines close to the axis. The kink waves lead to the transverse oscillations of spicules as a whole.
- Volume-filling Alfvén waves propagating from the photosphere upwards along magnetic field lines in the chromosphere. The Alfvén waves result in the oscillation of the ubiquitous magnetic field lines. These oscillations force the spicules to periodic displacement of their axes.
- Transverse pulses excited in the photospheric magnetic flux tube by means of buffeting of granules. The pulses may propagate upwards in the stratified atmosphere and leave "wakes" behind, which oscillate at the kink cut-off frequency of the stratified vertical magnetic flux tube. The wakes can be responsible for the observed $\geq$ 3-min period transversal oscillations in limb spicules.

It is important to estimate the energy flux stored in spicule oscillations. If the oscillations are caused by the waves excited by granulation, then the energy flux of waves should be in the range of the energy flux of granulation. The energy flux stored in an initial transverse pulse at the photosphere is $F \sim n_e c_k v_g^2$, where v_g is the granular velocity, say 1-2 km s^{-1}. Then, for the photospheric electron density of $2 \cdot 10^{17}$ cm^{-3} and Alfvén speed of 10 km s^{-1}, the estimated energy flux is $\sim 5 \cdot 10^8$ erg cm^{-2} s^{-1} (taking v_g as 1.25 km/s).
The same energy flux under chromospheric conditions (i.e. electron density of $2 \cdot 10^{11}$ cm^{-3} and Alfvén speed of 100 km s^{-1}) requires the wave velocity in the chromosphere to be about 125 km/s. This latter speed is by an order of magnitude higher than the observed value of oscillation velocity. This discrepancy can be resolved if the oscillations are caused by the wake behind a transversal pulse: in this case *almost the entire energy of the initial perturbation is carried by the pulse, while the energy of the wake is much smaller*. Therefore, even if the filling factor of magnetic tubes is 10%, the energy flux carried by pulses is more than enough to heat the solar chromosphere/corona.

6.1 Targets for future observations

More observations from space satellites and ground based coronagraphs are needed for a better and conclusive understanding of oscillatory events in solar limb spicules. There are few highlighted targets for future observations:

6.1.1 Phase relations between oscillations in neighbouring spicules

It is important to perform an analysis of phase relations between oscillations in neighbouring spicules. If spicule oscillations are caused by global Alfvén waves or they are

related to global photospheric oscillations, then the transverse displacement of spicules should show some spatial coherence i.e. a few neighbouring spicules should move in phase along the limb. Hinode/SOT time series in Ca II H and Hα lines seem to be an excellent data for such analysis work.

6.1.2 Phase relations between oscillations at different heights

A study the phase relation of transverse displacements of a particular spicule at different heights would allow us to infer whether the oscillations are due to standing or propagating wave patterns. Phase delays between different heights would determine the phase speed of perturbations, thus, the physical nature of the waves. Spectroscopic consecutive height series from ground based coronagraphs or time series of images from e.g. Hinode/SOT would allow to infer the wave length, phase speed or frequency of oscillations. These latter important diagnostic parameters may be then used to develop *spicule seismology* as suggested by Zaqarashvili et al. (2007).

6.1.3 Propagation of transverse pulse

Propagation of transverse pulses can be traced through a careful analysis of time series from e.g. Hinode/SOT. It is also important to search for oscillations of spicule axis at the kink or Alfvén cut-off frequency as estimated in the chromosphere. Polar macrospicules are probably the best targets for such work, as their life time is long enough when compared to the cut-off period.

Acknowledgements This paper review was born out of the discussions that took place at the International Programme "Waves in the Solar Corona" of the International Space Science Institute (ISSI), Bern. The authors thank for the financial support and great hospitality received during their stay at ISSI. The work of TZ was also supported by Georgian National Science Foundation grant GNSF/ST06/4-098. RE acknowledges M. Kéray for patient encouragement and is also grateful to NSF, Hungary (OTKA, Ref. No. K67746) and the Science and Technology Facilities Council (STFC), UK for the financial support received.

References

M. Abramowitz, A. Stegun, *Handbook of Mathematical Functions*, New York: John Wiley and Sons (1967).
J. Andries, E. Verwichte, B. Roberts, T. Van Doorsselaere, G. Verth, R. Erdélyi, Space Sci. Rev. **This Volume**, 30 pages (2009).
I. Ballai, R. Erdélyi, J. Hargreaves, Physics Plasmas, **1**3, 042108-1 (2006).
D. Banerjee, E. O'Shea, J.G. Doyle, Astron. Astrophys. **3**55, 1152 (2000).
J.M. Beckers, Solar Physics **3**, 367 (1968).
J.M. Beckers, Ann. Rev. Astron. Astrophys. **10**, 73 (1972).
J.D. Bochlin et al., The Astrophysical Journal **197**, L133 (1975).
B. De Pontieu, R. Erdélyi, Phil. Trans. Roy. Soc. A **364**, 383 (2006).
B. De Pontieu, R. Erdélyi, A.G. de Wijn, The Astrophysical Journal **595**, L63 (2003a).
B. De Pontieu, R. Erdélyi, S.P. James, Nature **430**, 536 (2004).
B. De Pontieu, T. Tarbell, R. Erdélyi, The Astrophysical Journal **590**, 502 (2003b).
B. De Pontieu et al., Science **318**, 1574 (2007a).
B. De Pontieu et al., PASJ **59**, S655 (2007b).
J.G. Doyle, J. Giannikakis, L.D. Xia, M.S. Madjarska, Astron. Astrophysics **431**, L17 (2005).
P.M. Edwin, B. Roberts, Solar Physics, **88**, 179 (1983).

R. Erdélyi, *Chapter 5. Waves and Oscillations in the Solar Atmosphere*, in (eds.) B.N. Dwivedi and U. Narain, *Physics of the Sun and its Atmosphere*, World Scientific, Singapore, pp.61-108 (2008).
R. Erdélyi, V. Fedun, Science **318**, 1572 (2007).
R. Erdélyi, C. Malins, G. Tóth, B. De Pontieu, Astron. Astrophysics, **467**, 1299 (2007).
B. Fleck, F.-L. Deubner, Astron. Astrophysics, **224**, 245 (1989).
B. Fleck, F. Schmitz, Astron. Astrophysics, **250**, 235 (1991).
T.G. Gadzhiev, G.M. Nikolsky, Sov. Astron. Lett. **8**, 341 (1982).
J. Hargreaves, PhD Thesis, The University of Sheffield (2008).
J. Hargreaves, R. Erdélyi, Astron. Astrophysics, **subm.**, 7 pages (2009).
S.S. Hasan, W. Kalkofen, The Astrophysical Journal **519**, 899 (1999).
S.S. Hasan, S.L. Keil, The Astrophysical Journal **283**, L75 (1984).
D.B. Jess, M. Mathioudakis, R. Erdélyi, P.J. Crockett, F.P. Keenan, D.J. Christian, Science, **in press**, 12 pages, (2009).
E. Khutsishvili, Solar Physics **106**, 75 (1986).
J. Koza, P. Sutterlin, A. Kucera, J. Rybak, APS conference series **368**, 75 (2007).
V. Kukhianidze, T.V. Zaqarashvili, E. Khutsishvili, Astron. Astrophysics **449**, L35 (2006).
V.I. Kulidzanishvili, G.M. Nikolsky, Solar Physics **59**, 21 (1978).
V.I. Kulidzanishvili, Y.D. Zhugzhda, Solar Physics **88**, 35 (1983).
C. Malins, R. Erdélyi, Solar Physics **246**, 41 (2007).
M.S. Madjarska, J.G. Doyle, J.-F. Hochedez, A. Theissen, Astron. Astrophysics **452**, L11 (2006).
P.M. Morse, H. Feshbach, *Methods of Theoretical Physics*, Vol. 1 (McGraw-Hill Book Company, Inc., New York, 1953).
Z.E. Musielak, P. Ulmschneider, Astron. Astrophysics **370**, 541 (2001).
G.M. Nikolsky, A.A. Sazanov, Sov. Astron. **10**, 744 (1967).
G.M. Nikolsky, A.G. Platova, Solar Physics **18**, 403 (1971).
N. Nishizuka, M. Shimizu, T. Nakamura, K. Otsuji, T.J. Okamoto, Y. Katsukawa, K. Shibata, The Astrophysical Journal (2009).
E. O'Shea, D. Banerjee, J.G. Doyle, Astron. Astrophysics **436**, L43 (2005).
A. Osin, S. Volin, P. Ulmschneider, Astron. Astrophysics **351**, 359 (1999).
P.G. Papushev, R.T. Salakhutdinov, Space Science Reviews **70**, 47 (1994).
S. Parenti, B.J.I. Bromage,G.E. Bromage, Astron. Astrophysics, **384**, 303 (2002)
J.M. Pasachoff, R.W. Noyes, J.M.Beckers, Solar Physics **5**, 131 (1968).
C.D. Pike and R.A. Harrison, Solar Physics **175**, 457 (1997).
C.D. Pike and H.E. Mason, Solar Physics **182**, 333 (1998).
I.C. Rae and B. Roberts, The Astrophysical Journal **256**, 761 (1982).
W.O. Roberts, The Astrophysical Journal **101**, 136 (1945).
B. Roberts, Solar Physics **61**, 23 (1979).
M.S. Ruderman, R. Erdélyi, Space Sci. Rev. **This Volume**, 36 pages (2009).
M.S. Ruderman, G. Verth, R. Erdélyi, The Astrophysical Journal **686**, 694 (2009).
F. Schmitz, B. Fleck, Astron. Astrophysics, **337**, 487 (1998).
E. Scullion, M.D. Popescu, D. Banerjee, J.G. Doyle, R. Erdélyi, Astron. Astrophysics, submitted, 16 pages, (2009)
P.A. Secchi, *Le Soleil*, vol. 2 (Gauthier-villas, Paris, 1877).
H.C. Spruit, Astron. Astrophysics **98**, 155 (1981)
H.C. Spruit and B. Roberts, Nature **304**, 401 (1983)
A.C. Sterling, Solar Physics **196**, 79 (2000).
G. Sutmann, Z.E. Musielak, P. Ulmschneider, Astron. Astrophysics **340**, 556 (1998).
Y. Taroyan, R. Erdélyi, Space Sci. Rev. **This Volume**, 26 pages (2009).
L.D. Xia, M.D. Popescu, J.G. Doyle, J. Giannikakis, Astron. Astrophysics **438**, 1115 (2005).
Y. Yamauchi, H. Wang, Y. Jiang, N. Schwadron, R.L. Moore, The Astrophysical Journal **629**, 572 (2005).
T. Van Doorsselaere, V.M. Nakariakov, E. Verwichte, The Astrophysical Journal **676**, L73 (2008).
G. Veth, R. Erdélyi, Astron. Astrophysics, **486**, 1015 (2008).
S.R. Weart, Solar Physics **14**, 310 (1970).
G.L. Withbroe, The Astrophysical Journal **267**, 825 (1983).
T.V. Zaqarashvili, E. Khutsishvili, V. Kukhianidze, G. Ramishvili, Astron. Astrophysics **474**, 627 (2007).

T.V. Zaqarashvili, N. Skhirtladze, The Astrophysical Journal **683**, L91 (2008).